Proceedings of the 11th International Conference on Fluid Flow, Heat and Mass Transfer (FFHMT 2024)
Chestnut Conference Centre - University of Toronto, Toronto, Canada – June 16-18, 2024
Paper No. 110
DOI: 10.11159/ffhmt24.110

Electrospray and Jet Contributions to the Current Measured during Electrospinning

Siavash Sarabi-Maneji, Jennifer Scott, Danny J.Y.S. Pagé
Royal Military College of Canada, Department of Chemistry and Chemical Engineering
Kingston, Ontario, Canada, K7K 7B4
Siavash.Sarabi-Mianeji@rmc.ca; Jennifer.Scott@rmc.ca; page-d@rmc.ca

Abstract - In this paper, measured current was shown to relate to the morphology of the filaments processed during electrospinning. In a series of experiments, a polycaprolactone-cellulose propionate blend in a THF-Methanol solvent system, was electrospun at potentials between 5 and 15 kV and a tip to collector distance of 12 cm. The electrical current was measured under all processed conditions and related to the observed filament morphology. In a step-approach, to better evaluate the current carried by the jet during electrospinning, the current generated by the solvent was measured separately from the current generated by the solution during electrospinning. The jet current obtained using this approach appeared to follow the trend predicted by the models referenced in this paper. The results indicated that solvent, segregated from the polymer solution jet during whipping, may carry most of the current under studied conditions at an applied potential above 10 kV, while the polymer solution jet carried most of the current at a lower applied potential. SEM results indicated that a potential of 8kV was sufficient to spin filaments at stable electrospinning processing conditions. At that applied potential, the smallest average diameter was obtained, also displaying the narrowest diameter distribution for the filaments. Overall, the results showed that measuring the current during electrospinning can be an effective tool in better understanding and predicting filament morphology.

Keywords**:** Electrospinning, electrospray, current, polycaprolactone, cellulose propionate, filaments

1. Introduction

As humanity increasingly faces challenges due to its impact on the global environment, it is striving to find more sustainable solutions to its consumption of natural and energy resources. Nanotechnology provides the opportunity to allow a more efficient use of materials by increasing the performance/mass ratio. It also provides the opportunity for a more sustainable processing of functional materials by decreasing the energy required for their processing. Electrospinning is a processing technique that has been used increasingly in the last three decades to produce materials with nanoscale attributes in the form of continuous filaments of diameters within the 10-1000 nm range. These spun filaments possess high surface area to volume ratio and are used increasingly to produce functional materials such as filters, membranes, scaffolds, and supports for catalysts [1, 2].

During electrospinning, an elevated potential (*i.e.*, 10-50 kV) is applied to a polymer melt or solution fed through needles, holes on a conductive surface, or a wetted drum [2]. As charges accumulate on the surface of the liquid, the electrical field is stretched, forming a continuous jet that is emaciated through a series of whipping actions until it reaches a grounded collector. By the time the jet completes its journey, usually measured in tens of centimetres, most of the solvent has left the jet, producing a polymer filament wound on the collecting surface.

The impact of several parameters on the electrospinning process have been studied, such as applied potential, tip to collector distance (TCD), flow rate, surface tension, viscosity, conductivity, measured current, ambient conditions, collector design, and solution feed system [1]. However, only a small fraction of literature studies provide data on the measured electrical current during processing. A simple internet search, performed on a commonly used platform, confirmed the increasing use of the electrospinning technique in research and processing [1,3]. Narrowing the search showed that less than 0.6% of the literature from the same pool made mentioned measuring the electrical current during processing [3]. Even when the current is measured, complete understanding of its impact on the electrospinning process is complicated by the lack of a thorough knowledge of the mass transfer mechanisms (*i.e.*, whipping and spraying) and their possible overlap occurring during the process [4].

The electrical current travelling with the polymer solution in the form of a jet during electrospinning is an important parameter as it relates to the movement of charges accompanying mass transport through the electrical field [5,6,7]. During processing, the current carried by the jet is a combination of surface charge advection and polymer solution bulk conduction, defined respectively in Eq. 1 where I is the electrical current, υ is the jet velocity, E is the electric field, σ_0 is the surface charge density, K is the electrical conductivity, and h is the radius of the jet [6].

$$I = 2\pi\sigma_0 h v + \pi E K h^2 \tag{1}$$

As the polymer solution is fed to the electrical field, the jet is initially larger, the bulk conduction current (resulting from the polymer solution jet conductivity) is dominant and can be approximated by the second term in the right-hand side of Eq. 1. As the jet travels through the field, free charges migrate to the surface of the jet due to charge repulsion, causing further stretching. The current travelling through the emaciated jet then becomes negligible in comparison to the current on the surface of the jet, which can be approximated with the first term on the right-hand side of Eq.1. By defining the jet volume flow rate as $Q = \pi h^2 \upsilon$, the current at the surface of the whipping jet can be estimated as $I = 2\sigma_0 Q/h$ [5].

Very few comprehensive models relate physical parameters applied to electrospinning [1, 5]. One of those models is known as the terminal jet theory [5]. Using the concept of jet instability [6,8], Fridrikh et al. modelled the polymeric jet as a cylindrical Newtonian fluid, stretched through a whipping motion [5]. The model predicts a final radius of the jet based on the competition between the surface tension and electrostatic repulsion forces on the surface of the jet coming to equilibrium. The model implies that whipping instability is the main factor in decreasing the jet diameter [5]. The terminal jet radius is defined in the following Eq. 2 [5]:

$$h_t = \left(\gamma \varepsilon \frac{Q^2}{I^2} \frac{2}{\pi(2\ln\chi - 3)}\right)^{1/3} \tag{2}$$

Parameters found in Eq. 2 are the surface tension γ, the permittivity of the surroundings ε, the volumetric flow rate Q, the current I, and the dimensionless wavelength parameter ratio χ, defined as the contour length of the jet over the radius of curvature of whipping. χ has also been approximated using the ratio of the length of the jet over the jet diameter in the initial straight segment before whipping occurs. In another version of Eq. 2, h_t was directly related to d_f, the spun filament diameter [9].

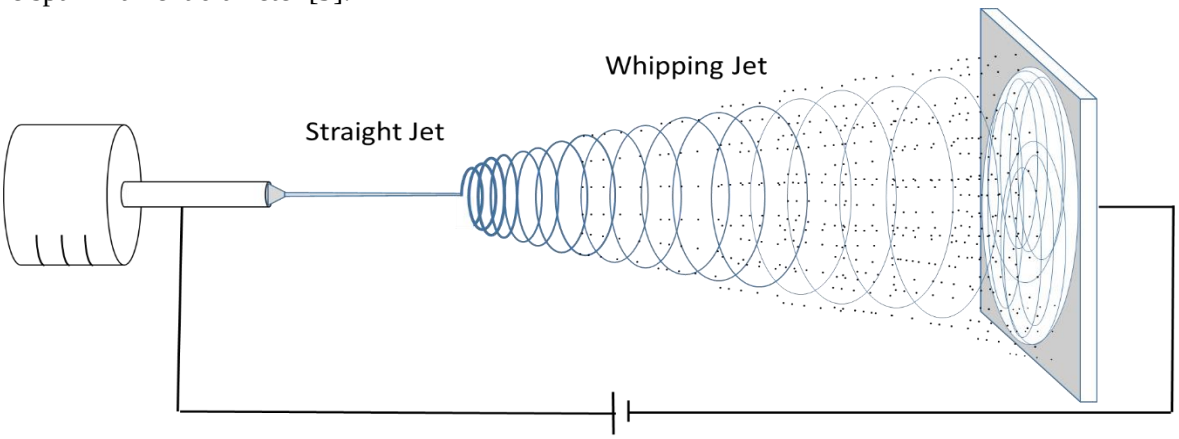

Fig. 1: Representation of a typical electrospinning process showing, left to right: syringe, needle, taylor cone, straight jet, onset of whipping, whipping jet, spray of solvent droplets segregating from the jet, collector, and high potential source at the bottom.

In addition to travelling through and on the surface of the jet, the electrical current measured during electrospinning may also include a third component, which is due to the solvent segregating from the solution contained in the jet and

forming a spray of charged droplets travelling independently to the collector, as depicted in Figure 1 [4]. Although three components to the measured current have been recognized, quantification of the current traveling independently with the the whipping jet and the sprayed solvent during electrospinning has remained elusive.

This paper presents a step approach to estimate the contribution of each polymer solution jet and solvent spray to the the current generated during electrospinning over a range of applied potential. The study was performed using a 20% equal blend of polycaprolactone (PCL) and cellulose propionate (CP) in a solvent mixture of 1:3 methanol (MeOH) in tetrahydrofuran (THF). The cellulose propionate was selected for its low toxicity and to improve the mechanical properties of PCL, a polymer used in many biomedical applications.

2. Methodology

2.1. Materials

Capa TM 6500 is a biodegradable polyester purchased from Perstorp and used as the polycaprolactone source with an average MW = 50 000 g/mol, a melting point of 60 ^{o}C and a T_g of -60 °C. Cellulose propionate is a modified agro-polymer, with an average MW ~130,000 g/mol, purchased from Aldrich.

MeOH (99.8%) and THF (99%) were purchased from Caledon Lab. Equal amounts of each polymer were weighed to obtain a total concentration of 20% w/v in a solvent mixture of 1MeOH:3THF by volume. The resulting solution was mixed using a magnetic stir bar at room temperature for 48 hours and then used for electrospinning.

2.2. Solution surface tension

Surface tension was measured using a DuNouy Tensiometer. A 10 mL beaker was used as the sample container and the platinum ring was immersed in the solution. The amount of force needed to overcome the surface tension of the solution was measured. Each solution was measured three times.

2.3. Electrospinning

A power supply (PS375/+20KV, Stanford Research System) was used to create a DC voltage from 5 to 15 kV. A 5 mL glass syringe with an 18 G flat-tip needle was used as a sample container/feeder. A syringe pump (Fisher Scientific) was used to maintain the desired flow rate. The positive electrode from the power supply was attached to the needle and the negative electrode was attached to the grounded collector, a rotating drum with a speed of 100 rpm covered with aluminum foil. The current was measured using a picoammeter from IX Innovations, Model PocketPico P110, connected in series.

2.4. Scanning Electron Microscopy

The diameter and morphology of the electrospun polymer filaments were analyzed using a Philips VP-30XL scanning electron microscope at an accelerating voltage of 15 kV. Aluminum foil was used for collecting the spun filaments. Collected samples were cut in a rectangular shape and fixed to carbon tape. SEM images with magnification of 5000x and the Image J software were used to measure filament diameter. Three images over three different samples were analyzed, resulting in a minimum of 100 measurements for each studied condition.

3. Results and Discussion

A 20% w/v solution of PCL/CP in a solvent blend of 1MeOH:3THF by volume was processed by electrospinning at potentials of 5-15 kV, a tip to collector distance (TCD) of 12 cm, and a flow rate of 0.5 mL/h. Figure 2 shows sample SEM micrographs (left) and corresponding filament diameter distribution (right) for spun filaments at 5 kV (top), 8 kV (middle), and 15 kV (bottom). The sample micrographs clearly show that filaments, with a smooth surface and no beading, were obtained under the studied conditions. The filament diameters are reported from 100 measurements for each population taken over a minimum of three micrographs for each set of process parameters. Although filaments are obtained under all reported conditions, the filament diameter distribution varied considerably. The distribution is broad for the filament populations obtained at 5 kV and 15 kV, extending to larger values for the higher potential. The diameter distribution is much narrower for the filament population obtained at 8 kV.

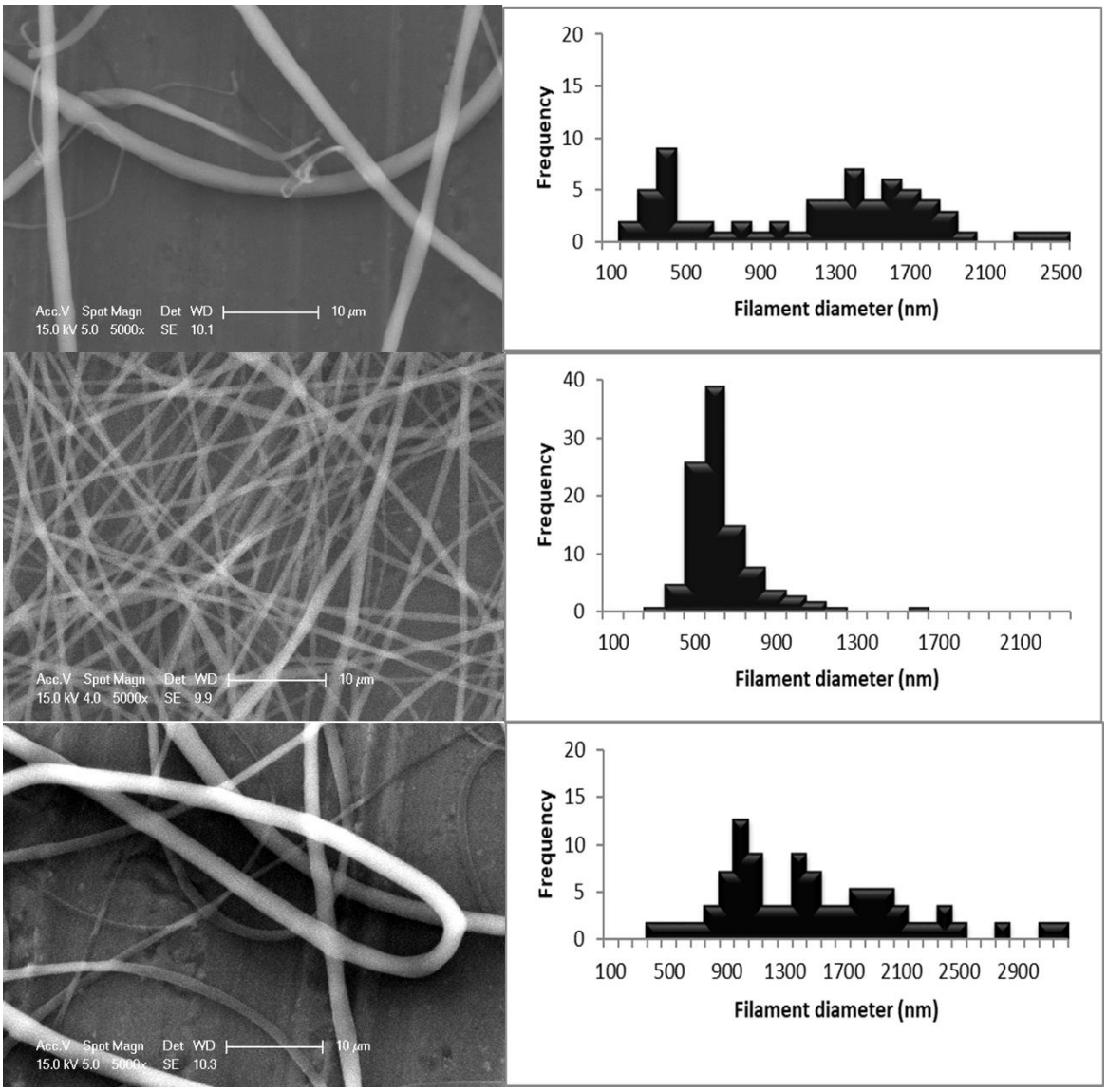

Fig. 2: PCL/CP filaments processed at a tip to collector distance (TCD) of 12 cm and a flow rate of 0.5 mL/h. SEM micrographs (left) and corresponding filament diameter distribution (right) for spun filaments obtained at 5 kV (top), 8 kV (middle), and 15 kV (bottom).

Figure 3 shows the trend of the average filament diameter as a function of the applied potential (left), where each error bar represents the standard deviation of 100 measurements taken over three sample micrographs. On the right side of Figure 3, a corresponding sample of current measurements, over a period of 50 seconds, is provided for each applied potential. With exception to the condition for an applied potential of 5 kV, the average filament diameter increases as a function of applied potential and the measured current increased as a function of applied potential for all conditions. In regards to the results at 5 kV, the top left micrograph of Figure 2 and the sample current at the bottom right of Figure 3 show variations in filament diameter and measured current close to one order for each. These results indicate an electrical field that is too weak to sustain an electrospinning process at steady state.

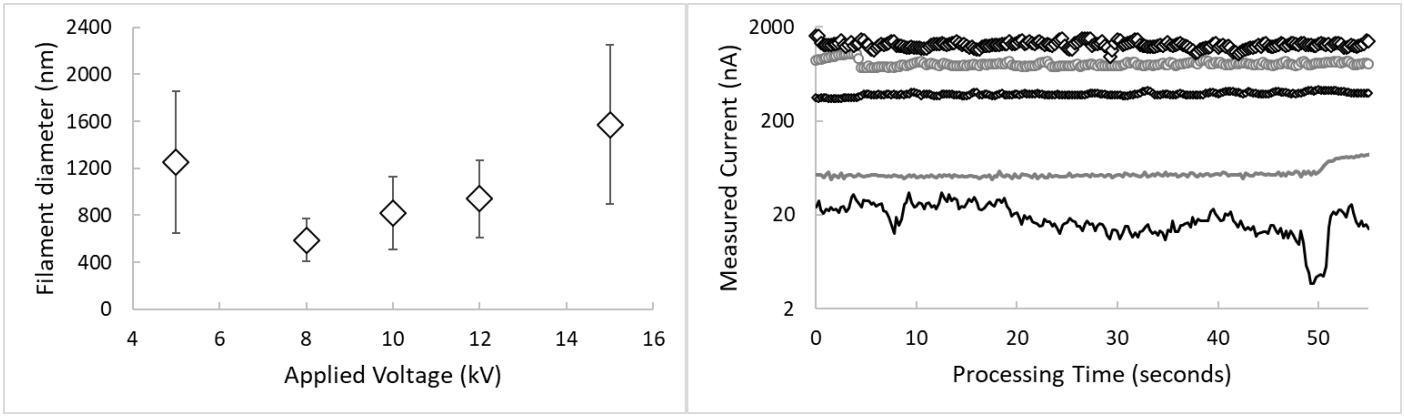

Fig. 3: Average spun PCL/CP filament diameter as a function of applied potential (left). Each error bar represents the standard deviation of 100 measurements. Sample current measurements (right) taken during spinning at a TCD of 12 cm and applied potentials of 5, 8, 10, 12, and 15 kV starting from the bottom.

The left side of Figure 4 shows a linear relationship for the measured current as a function of the applied potential starting from 8 kV onward for a TCD of 10 cm and 12 cm. The points at 5 kV fall out of linearity as they do not represent stable electrospinning conditions. The linearity of the results suggests that a minimum threshold of applied potential, close to 8 kV, is required to achieve stable electrospinning within the TCD and feed flow conditions selected. The right side of Figure 4 shows that the flow rate has no significant impact on the measured current for the studied conditions. The horizontal lines represent the calculated current from linear equations appearing on the left side of Figure 4.

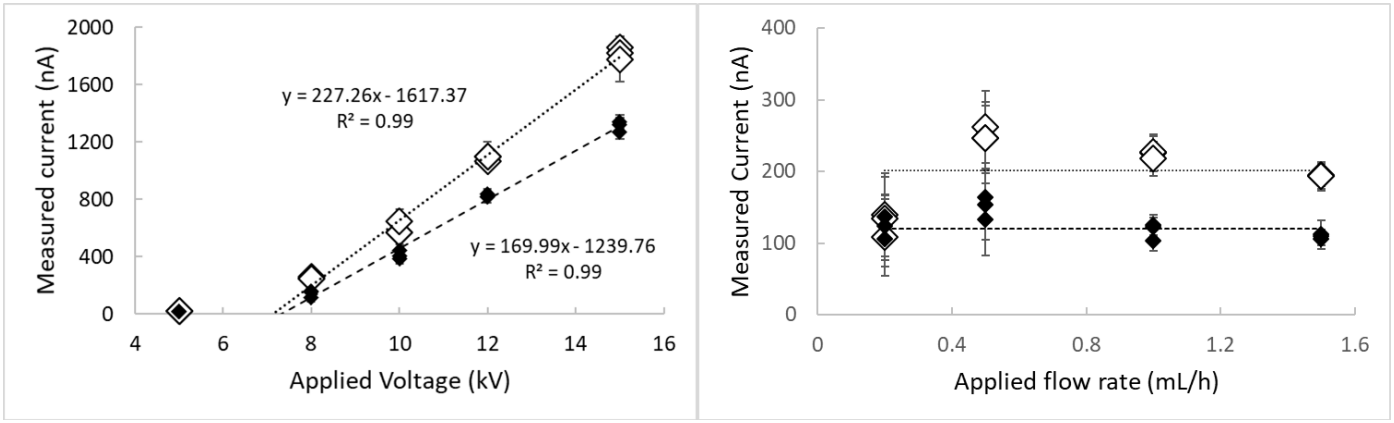

Fig. 4: Measured current over three spinning runs as a function of applied potential (left) at a flow of 0.5 mL/h at 10 cm (white) and 12 cm (black) TCD. Measured current as a function of flow rate (right) at a potential of 8 kV at 10 cm (white) and 12 cm (black) TCD.

Table 1 compares the measured current, from electrospinning at a TCD of 12 cm, a flow rate of 0.5 mL/h, and applied potentials from 5 kV to 15 kV, with the current calculated from each term of Eq. 1 using the diameter of the initial jet taken at 3 mm from the tip of the needle. Other parameters used were solution conductivity K = 0.001 S/m and surface charge density $\sigma_0 = \varepsilon E$.

With exception to the conditions at 5 kV, previously defined as insufficient to sustain electrospinning at steady state, the bulk current calculated with Eq.1 using the measured radius are comparable in scale to the measured current. The calculated surface current values are four orders of magnitude smaller in size which is consistent with previous research that reported that bulk conductivity dominates over surface conductivity in the initial straight jet [5].

Table 1: Measured and calculated current from initial jet for TCD of 12 cm and flow rate of 0.5 mL/h.

Applied Potential (kV)	Measured Current (nA)	Jet diameter 3 mm from tip (μm)	Bulk current Eq. 1 (nA) [6]	Surface current Eq. 1 (nA)
5	22 ± 2	66 ± 25	143 ± 108	0.035 ± 0.013
8	144 ± 21	75 ± 10	257 ± 69	0.053 ± 0.007
10	412 ± 29	78 ± 13	398 ± 132	0.059 ± 0.010
12	824 ± 30	94 ± 22	694 ± 324	0.059 ± 0.013
15	1310 ± 36	106 ± 24	1020 ± 462	0.068 ± 0.015

While the principles of conservation of mass and charge for the jet can be fair assumptions in the initial part of the electrospinning process, it was proposed that solvent evaporation from the jet before it reaches the collector may present additional challenges [5]. Using superimposed independent electrodes at the collector, Bhattacharjee et al. [4] provided evidence of solvent segregation from the jet, resulting in a separate current contribution to the one generated by the jet. In their experiment, the jet was collected on one electrode while the segregated solvent was assumed to reach both electrodes [4].

This paper used a complementary approach to the one described above, by assuming that all of the solvent leaves the jet by the time it forms a filament on the collector, and estimated that the solvent, in its entirety, generated current by electrospray separately from the jet. Using this last assumption, the current generated by only the solvent was measured at a flow rate of 0.4 mL/h, which corresponds to the amount of solvent contained in the polymer solution used for electrospinning. In Figure 5, measured current is reported as a function of applied potential for electrospinning with a 20% polymer solution, at 0.5 mL/h, and electrospraying with the solvent only, at 0.4 mL/h. The electrospray current is consistently below that of the electrospinning current. The differences between the two data sets are also plotted and, consistent with the assumption made above, are estimated to be the current carried by the jet during electrospinning, independent from the segregated solvent. As explained further down, the general trend is also consistent with Eq.2.

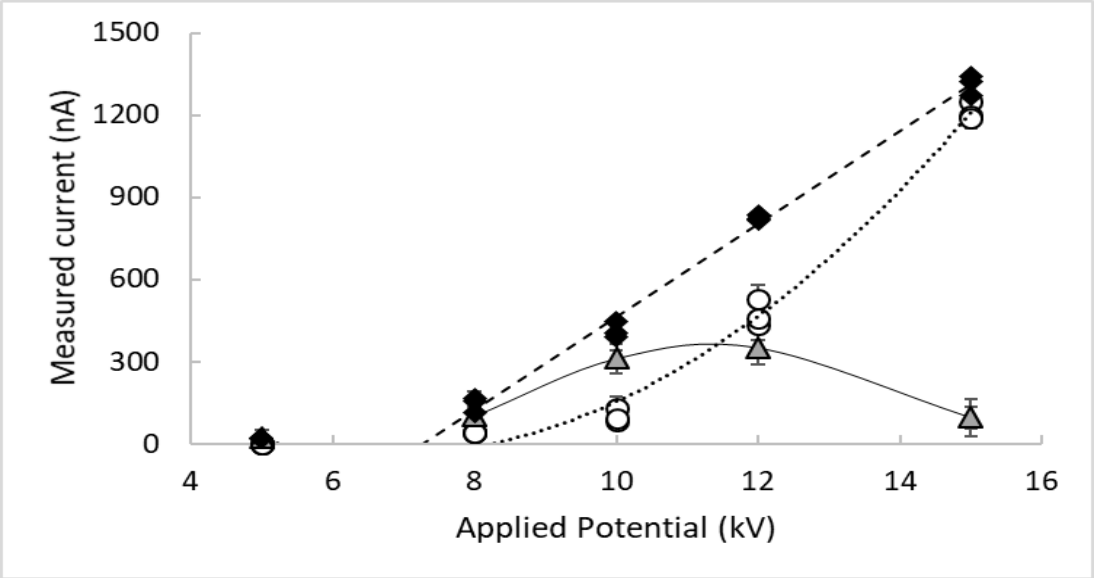

Fig. 5: Measured current in triplicates for electrospinning with a 20% polymer solution at 0.5 mL/h (black diamonds), electrospraying with solvent only at 0.4 mL/h (white circles) as a function of applied potential at TCD of 12 cm. Lines represent trends. The gray triangles are the differences between the averages of the electrospinning and electrospray current data sets and are attributed to the current carried by the terminal jet in this paper.

Figure 5 supports the observed trend of increasing filament diameter as a function of applied potential under steady-state electrospinning conditions. At 8kV and 10 kV, less solvent segregates from the jet and therefore more solvent is present present with the polymer in the jet. As potential is increased to 12 kV and 15 kV, more solvent segregates from the jet, limiting its stretching and resulting in larger filament diameters. Jet stretching may be affected in two ways by the loss of of solvent. First, the evaporating solvent may remove charges from the surface of the jet, reducing the amount of stretching stretching caused by charge repulsion [4]. Second, the escaping solvent would increase the viscosity within the jet and offer more resistance to stretching of the jet [9].

Calculated terminal jet currents, using Eq. 2, are reported in Table 2. The measured filament diameters are also reported, from which the terminal jet radius is determined, (other parameters are the flow rate, the permittivity of air, the surface tension of the solution mixture measured as 0.0296 kg/s^2, and the dimensionless wavelength parameter χ taken as the initial jet length over its diameter [10]) with a value of 74 ± 10 nm. The calculated terminal jet currents, from Eq. 2, are generally less than half of those proposed by the triangles in Figure 5 and follow a similar trend.

Table 2: Calculated surface charge density (σ) and surface current for terminal jet at TCD of 12 cm and flow rate of 0.5 mL/h.

Applied Potential (kV)	Meas. filament diameter (nm)	Surface current Eq. 2 (nA) [5]	$\sigma = 2\varepsilon\Delta Vk$ (C/m^2) [11]	Surface current Eq.1 (nA) [6]
5	1253 ± 603	34 ± 12	9.89E-05	44
8	589 ± 181	106 ± 29	3.37E-04	318
10	820 ± 310	70 ± 20	3.18E-04	227
12	940 ± 328	51 ± 11	3.10E-04	179
15	1573 ± 676	24 ± 8	2.36E-04	84

The last column in Table 2, takes a closer look at the resulting jet surface current using Eq. 1. In order to perform the calculation, an appropriate surface charge density must be determined. The definition of surface charge density for a plane surface, using the permittivity of air and the electrical field, $\sigma = \varepsilon E$, is not adequate and results in jet surface current values three orders of magnitude smaller than the current values attributed to the jet in Figure 5. Hohman et al. demonstrated the importance of the accumulation of charge density on the surface of the jet and its impact on both the electrical fields normal and tangential to the jet, causing the instability responsible for the onset of whipping [6]. Enze demonstrated theoretically the impact of an increased surface curvature on producing a higher surface charge density [11]. Although the model proposed by Enze has limitations in its application, as pointed out by Bhattacharya, as it depends on the determination of ΔV near the surface [12], it still captures two important aspects with relevance to electrospinning, 1) the role of surface curvature on increasing charge density and 2) the relation of surface charge density with the electrical field near the surface of the jet. A high surface charge density would contribute to a strong electrical field normal to the jet surface that would strip charged solvent droplets from the jet, contributing to the overall electrospinning current by electrospray, which is consistent with current trends presented in Figure 5.

The surface charge density values, found in the fourth column of Table 2, were calculated using a fraction (0.0007) of the applied voltage as ΔV, and the reciprocal of the filament radius 1/h as the curvature k. The resulting jet surface current values are provided in the last column of Table 2. Although not a perfect fit, they relate in size and general trend to the experimentally sourced values, attributed to the jet, in Figure 5.

4. Conclusion

In conclusion, this paper showed that measuring the current during electrospinning can be an effective tool in better understanding and predicting filament morphology. The electrical current was measured under all processing conditions as a function of the applied potential and flow rate. SEM micrographs indicated that a potential of 8 kV was sufficient to spin filaments with stable processing conditions and a regular morphology. At that applied potential, the smallest average diameter was obtained, also displaying the narrowest diameter distribution for the filaments. In a step-approach, to better evaluate the current carried by the jet during electrospinning, the current generated by the solvent was measured separately

from the current generated by the solution during electrospinning. The jet current obtained, with the approach presented, appeared to follow the trend predicted by the models referenced in this paper. The results indicated that solvent from the polymer solution jet during whipping, may carry most of the current under studied conditions of an applied above 10 kV, while the polymer solution jet may carry most of the current at a lower applied potential. Solvent from the jet during electrospinning would support the observed trend of larger filament diameters obtained when spun higher applied potential.

Acknowledgements

The authors would like to thank the Canadian Defence Academy Research Program and the AUTO21 of the Ontario Centre of Excellence for their financial support. Also, Mr. C. McEwen and Mr. B. Ball for their technical support with the processing equipment and Dr. J. Snelgrove with the SEM analysis.

References

[1] Y. Guo, X. Wang, Y. Shen, K. Dong, L. Shen, and A.A.A. Alzalab, "Research progress, models and simulation of electrospinning technology: a review", *J. Mater. Sci.*, vol. 57, pp.58-104, 2022.

[2] B.A. Venmathi Maran, S. Jeyachandran, and M.A. Kimura, "Review on the Electrospinning of Polymer Nanofibers and Its Biomedical Applications", *J. Compos. Sci.*, vol. 8, no. 32, pp.1-19, 2024.

[3] Internet search, by D. Page, using the Google Scholar search engine, counted 588 000 literature items mentioning "electrospinning", thus confirming the wide use of the technique in research. The search was then refined by adding the terms "measured current" or "current measurement" reducing the number of literature items obtained to 3 510; 8 December 2023.

[4] P.K. Bhattacharjee, T.M. Schneider, M.P. Brenner, G.H. McKinley, and G.C. Rutledge, "On the measured current in electrospinning", *J. Appl. Phys.*, vol. 107, 044306, pp. 1-7, 2010.

[5] S.V. Fridrikh, J.H. Yu, M.P. Brenner, and G.C. Rutledge, "Controlling the fiber diameter during electrospinning", *Phys. Rev. Lett.*, vol. 90, 144502, pp.1-4, 2003.

[6] M.M. Hohman, M. Shin, G.C. Rutledge, and M.P. Brenner, "Electrospinning and electrically forced jet. I. Stability theory", *Phys. Fluids*, vol. 13, pp. 2201-2220, 2001.

[7] M.M. Hohman, M. Shin, G.C. Rutledge, and M.P. Brenner, "Electrospinning and electrically forced jet. II. Applications", *Phys. Fluids*, vol. 13, pp. 2221-2236, 2001.

[8] A.L. Yarin, S. Koombhongse, and D.H. Reneker, "Taylor cone and jetting from liquid droplets in electrospinning of nanofibers", *J. Appl. Phys.*, vol. 90, pp. 4836-4846, 2001.

[9] M.M. Munir, A.B. Suryama, F. Iskandar, and K. Okuyama, "Scaling law on particle-to-fiber formation during electrospinning", *Polymer*, vol. 50, pp. 4935-4943, 2009.

[10] A. Baji, Y.-W. Mai, S.-C. Wong, M. Abtahi, and P. Chen, "Electrospinning of polymer nanofibers: Effects on oriented morphology, structures and tensile properties", *Compos. Sci. Tech.*, 70, pp. 703-718, 2010.

[11] L. Enze, "The distribution function of surface charge density with respect to surface curvature", *J. Phys. D.: Appl. Phys.*, vol. 19, pp. 1-6, 1986.

[12] K. Bhattacharya, "On the dependence of charge density on surface curvature of an isolated conductor", *Phys. Scr.*, vol. 91, 035501, pp.1-8, 2016.